Mathematical Model of Static and Dynamic Recrystallization, Roll Force and Mean Flow Stress of the Nb-Microalloyed Steels for Plain Steel Hot Roughing Mill

Digital technologies are transforming industry at all levels. Steel has the opportunity to lead all heavy industries as an early adopter of specific digital technologies to improve our sustainability and competitiveness. This column is part of AIST's strategy to become the epicenter for steel's digital transformation, by providing a variety of platforms to showcase and disseminate Industry 4.0 knowledge specific for steel manufacturing, from big-picture concepts to specific processes.

Authors

M.L.P. Machado
Instituto Federal do Espírito Santo, Vitoria, ES, Brazil
marcelolucas@ifes.edu.br

J.G. Santos
ArcelorMittal Tubarão, Serra, ES, Brazil
juliana.gomes@arcelormittal.com.br

In order to produce steels with higher added value and to meet market needs for greater strength, lower weight and lower cost, industries are increasingly striving to know all the relationships between operational parameters and the metallurgical and final steel properties. To support this process, mathematical models represent a major technological advance. They are capable of predicting the final mechanical properties and microstructural evolution of a steel alloyed from the chemical composition and process conditions.

This study proposes a mathematical model capable of predicting the rolling force and austenitic grain size, following the methodology defined in the literature, considering parameters such as drawing and roughing temperatures, strain rates, interpass time, types and recrystallization fractions, and geometric relations of the rolling mill.

Materials and Methods

To predict the rolling force and the austenite grain size based on the mean flow stress, a mathematical model was developed in a spreadsheet considering the equations from literature for Nb-microalloyed steels and industrial data from a plain steel hot roughing mill.

The chemical composition range was considered according to Table 1.

Table 1

Chemical Composition of Steel (wt.%)

C	Mn	P	S	Al	Nb
0.080	0.600	0.020	0.010	0.045	0.032

Table 2

Equations Used in the Mathematical Model

SRX — Static recrystallization	MDRX — Metadynamic recrystallization
For high-Nb steel $t_{0.5SRX} = (-5.24 + 550Nb) \times 10^{-18} \varepsilon^{(-4+77Nb)} d_0^2 \exp\left(\frac{330,000}{RT}\right)$ (Eq. 1)	For high-Nb steel $t_{0.5MDRX} = 4.42 \times 10^{-7} \dot{\varepsilon}^{(-0.59)} \exp\left(\frac{153,000}{RT}\right)$ (Eq. 2)
For microalloyed steel $t_{0.5SRX} = 1.57 \times 10^{-14} d_0^2 \varepsilon^{-2.9} \exp\left(\frac{271,000}{RT}\right)$ (Eq. 3)	For microalloyed steel $t_{0.5MDRX} = 1.84 \left[\dot{\varepsilon} \exp\left(\frac{330,000}{RT}\right)\right]^{(-0.86)} \exp\left(\frac{271,000}{RT}\right)$ (Eq. 4)
$X_{SRX} = 1 - \exp\left[-0.693\left(\frac{t_{ip}}{t_{0.5}}\right)\right]$ (Eq. 5)	$X_{MDRX} = 1 - \exp\left[-0.693\left(\frac{t_{ip}}{t_{0.5}}\right)\right]$ (Eq. 6)
For T>950°C $d_{SRX} = 1.1 d_0^{0.67} \varepsilon^{-0.67}$ (Eq. 7)	$d_{MDRX} = 1,370 \varepsilon^{-0.13} \exp\left(-\frac{45,000}{RT}\right)$ (Eq. 8)
$d = d_{SRX} \cdot X^{4/3} + d_{i-1} \cdot (1 - X)^2$ (Eq. 9)	$d^{4.5} = d_{MDRX}^{4.5} + 4.1 \cdot 10^{23} t_{ip} \exp\left(\frac{-435,000}{RT}\right)$ (Eq. 10)

The recrystallization kinetics for hot-rolled high-Nb steel and microalloyed steels (C-Nb) can be given by Eqs. 1–10, as summarized in Table 2. Those equations were developed and adjusted by Hodgson, Roucoules and Kirihata.[1,2]

where

$t_{0.5SRX}$ and $t_{0.5MDRX}$ = time to obtain the fractional recrystallization,
ε = strain,
$\dot{\varepsilon}$ = strain rate,
X_{SRX} and X_{MDRX} = fractional recrystallization and
d_{SRX} and d_{MDRX} = austenitic grain size.

Eq. 10 is used to calculate final austenitic grain size after full recrystallization and Eq. 9 is used to calculate final grain size when recrystallization fraction is less than 0.95.

The strains are calculated according to the following equations:

$$\varepsilon = 2/\sqrt{3} \cdot \ln\left(\frac{h1}{h2}\right) \quad \text{(Eq. 11)}$$

$$\dot{\varepsilon} = \frac{\varepsilon}{t} \quad \text{(Eq. 12)}$$

$$\varepsilon r = \frac{1}{2} tg(\phi n) \quad \text{(Eq. 13)}$$

where

$h1$ = thickness of the previous pass (mm),
$h2$ = thickness of the pass (mm),
t = time of application of the deformation in the contact arc (s),
ϕn = Neutral angle (radians) and
εr = redundant strain.

Process parameters such as plate thickness (225 mm) and numbers of passes (five) were set to form the comparative basis of the mathematical model in order to keep coherence between the input data and the results obtained, according to Tables 3 and 4.

where

ε = strain,
$\dot{\varepsilon}$ = strain rate,
εr is redundant strain,
MFS is mean flow stress and
Ks is supersaturation ratio (driving force to niobium precipitation). It can be obtained from Eq. 14:

$$Ks = \frac{10\left(\frac{2.26 - 6,770}{T_{RH}}\right)}{10\left(\frac{2.26 - 6,770}{T}\right)} \quad \text{(Eq. 14)}$$

where

T_{RH} = charging temperature of material (K) and
T = temperature in the pass (K).

There are models that calculate the mean flow stress (TEM) in C-Mn steels during hot strip mill. The model developed by Misaka and Yoshimoto, Eq. 15,[3,4] was the one that best fit the hot rolling.

To consider other alloyed contents and static and dynamic recrystallization, it was necessary to make improvements in the Misaka's equation shown in Eqs. 16 and 17.

Table 3

Input Variables

ID	Slab thickness (mm)	Temp (ºC)	Width (mm)	P measure (ton) (roll force)	Roll speed (RPM)
1	225	1,194	1,427	2,319	26.01
2	225	1,211	1,400	1,965	27.59
3	225	1,188	1,446	2,597	27.50
4	225	1,203	1,439	2,369	27.50

Table 4

Output Variables

ID	ε	$\dot{\varepsilon}$ (s^{-1})	Ks	εr	MFS_{mod} final (MPa)
1	0.274253	2.71	0.905	0.051082	70.622
2	0.274253	2.79	1.029	0.052209	69.561
3	0.274253	2.78	0.905	0.052116	71.074
4	0.274253	2.78	0.949	0.052129	69.549

Equation 15

$$TEM_{MK} = \exp\left[0.126 - 1.75[\%C] + 0.594[\%C]^2 + \frac{2,851 + 2,968[\%C] - 1,120[\%C]^2}{T}\right] \cdot \varepsilon^{0.21} \cdot \dot{\varepsilon}^{0.13}$$

$$TEM\text{Nb Cor} = TEM_{MK}\{0.768 + 0.51[\text{Nb}] + 0.137[\text{Mn}] + 4.217[\text{Ti}]\} \quad \text{(Eq. 16)}$$

$$TEM_{MOD} = TEM_{COR}(1 - X_{dyn}) + \text{Kc}\sigma_{ss} X_{dyn} \quad \text{(Eq. 17)}$$

In order to predict the mean flow stress of the steels as a function of temperature and carbon content, the equation developed by Misaka and adjusted by Minami et al.[5] to consider microalloyed steels. To calculate the applied roll force, Machado[1] developed Eq. 18 based on the Sims model.

$$P = \frac{TEM_{MOD} \cdot W \cdot \sqrt{R'(h1 - h2)Q}}{9,800} \quad \text{(Eq. 18)}$$

where

P = load or rolling force of the working cylinder (ton),
TEM_{MOD} = final mean flow stress of the model in the pass considered (MPa),
W = initial strip width (mm),
R' = deformed radius (mm),
$h1$ = thickness of the previous pass (mm),
$h2$ = thickness of the pass (mm) and
Q = geometric factor.

The equations developed by Palmiere, Gladman, and Siciliano[6–8] were used to obtain the dissolution temperature of the steel, according to equations shown in Table 5. The solubilization of Nb, as well as other microalloying elements during austenitization, is essential for the steels to reach the expected mechanical properties.

Two specimens (top and tail) were removed from sketch for microstructural characterization. The specimens were sanded and polished. They were then treated with a reagent consisting of an aqueous solution of picric acid (3 g) and hydrochloric acid (3 ml) around 1 minute.

The austenitic grain size measurement was realized in the two samples, using manual techniques, tracing a line to measure the grains that were well defined by microscope software.

A flowchart was elaborated, according to Fig. 1, with the routine of calculation of the mathematical model used to obtain the deformations, recrystallization fraction and grain size. For the purpose of calculation, it was considered that the material was completely recrystallized when the recrystallization fraction reached a value of ≥95%.

Table 5

Dissolution Temperature of the Solubility Product of Nb Precipitates

Authors	Equations
Gladman	$\log([\text{Nb}][\text{C}]) = 2.26 - 6,770\text{T}^{-1}$ (Eq. 19)
	$\log([\text{Nb}][\text{C}]) = 3.42 - 7,900\text{T}^{-1}$ (Eq. 20)
	$\log([\text{Nb}][\text{C}]) = 2.96 - 7,510\text{T}^{-1}$ (Eq. 21)
Palmiere	$\log([\text{Nb}][\text{C}]) = 3.04 - 7,290\text{T}^{-1}$ (Eq. 22)
	$\log([\text{Nb}][\text{C}]) = 3.70 - 9,100\text{T}^{-1}$ (Eq. 23)
	$\log([\text{Nb}][\text{C}]) = 3.18 - 7,700\text{T}^{-1}$ (Eq. 24)
Siciliano	$\log([\text{Nb}][\text{C}]) = 2.26 - 6,770\text{T}^{-1}$ (Eq. 25)
	$\log([\text{Nb}][\text{C}]) = 4.09 - 10,400\text{T}^{-1}$ (Eq. 26)
	$\log\left([Nb]\left[C + \frac{12}{14} \cdot N\right]\right) = 2.26 + \left(838[Mn]^{0.246} - 1,730[Si]^{0.594} - 6,440\right)T^{-1}$ (Eq. 27)

Results

All results were calculated for four coil thickness. For example: R1 = pass 1, R2 = pass 2 and so on.

- Roll force: As the choice of the equations to be used in the model is of fundamental importance, the calculations of

Figure 1

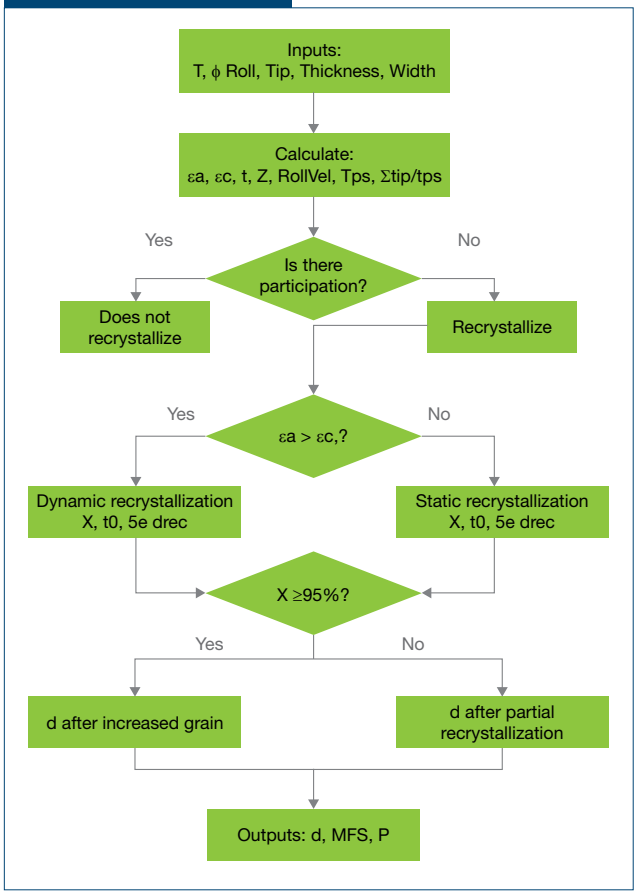

Flowchart of the calculation routine of the mathematical model.

roll force were realized and compared using equations for high-Nb steel and microalloyed steel.

Figs. 2–5 show the calculated values of roll force are more consistent using the equations for high-Nb steels than for microalloyed steels.

- Mean flow stress (MFS): The MFS based on the Sims model, which uses actual roll force data from the industry, was compared to calculated by mathematical model, obtained from the Misaka equation and its adjustments. Figs. 6–9 show that the model is consistent in the MFS calculation and followed a trend very similar to the Sims results in all coil thicknesses.
- Austenitic grain size: It was considered that the limit between the austenitic grains is the ferrite (white color) and the pearlite (black color), since the ferrite nucleation occurs in the previous grain boundary and pearlite is obtained by the normal process of phase transformation (diffusion), considering that the specimen was air-cooled, according to Fig. 10.

The mean grain size of the samples was 88 µm and the final grain size predicted by the model was on average 100 µm.

Discussion

The model showed that it is consistent in the calculation of the roll force, since it followed the same tendency in all the coil thicknesses. The average

Figure 2

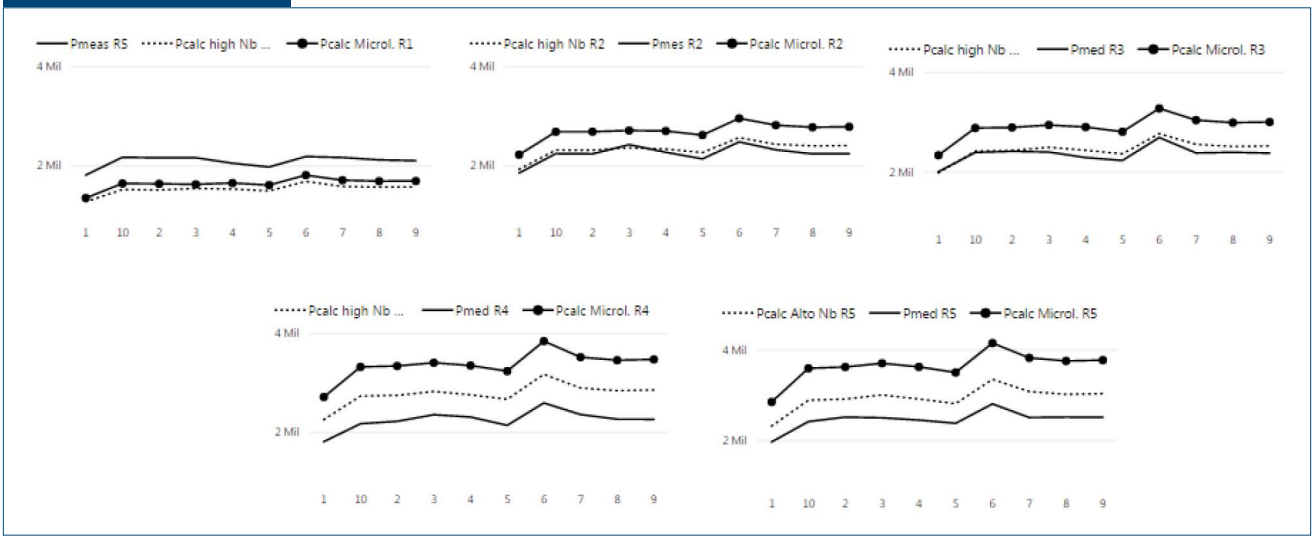

Comparison between roll force measured x calculated by the model using equations considering high-Nb steel and microalloyed steels for thickness of 34 mm. Unit of measurement of the graphs in tons.

Figure 3

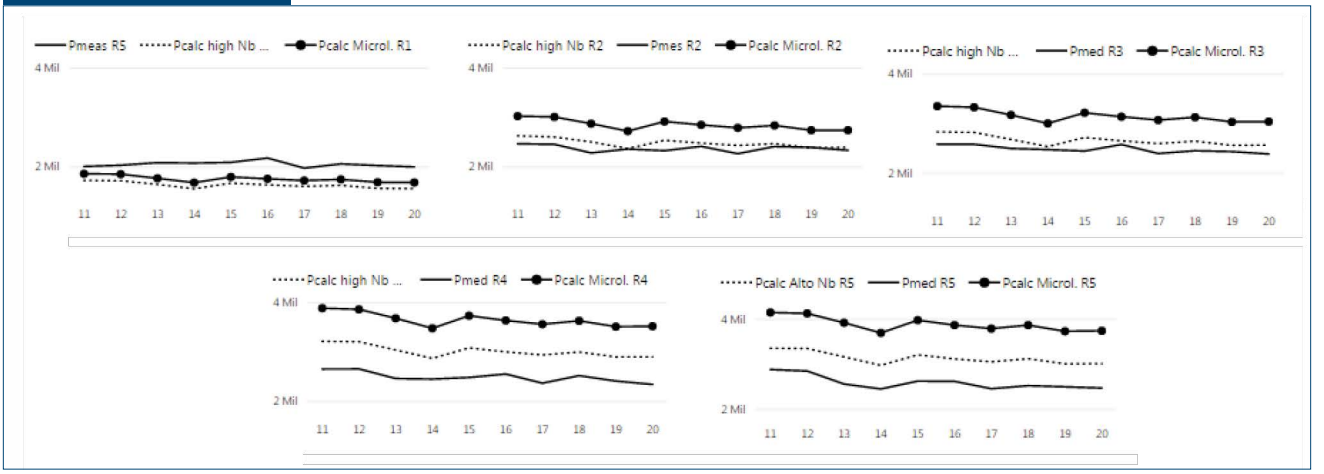

Comparison between roll force measured x calculated by the model using equations considering high-Nb steel and microalloyed steels for thickness of 36 mm. Unit of measurement of the graphs in tons.

deviation between the measured and calculated roll force was on average 15%. The mechanism of material softening in the first pass was static and in the other passes was dynamic.

A reversal in the results of MFS in pass 1 (R1) can be observed when compared to the other passes (R2 to R5), where the MFS of Sims is greater than the MFS of the model. This is consistent with the actual roll force at pass 1 being larger than that calculated by the model. The mean deviation between the actual MFS and the calculated MFS was on average 15% per pass.

Variable width impacted the roll force during the roughing mill. An increased width impacts a larger area to be deformed, increasing the time of application of the force and deformation of the work roll. The width of the plates ranged from 1,000 to 1,500 mm in the study data.

The temperature had no impact on the increase of the force during the roughing mill. This can be explained by the high temperatures in which the material is in this process, with a minimum temperature of 1,114°C and a maximum of 1,228°C in the study data. The average temperature loss in each pass was around 20°C, maintaining the stable temperature during the roughing mill.

The maximum dissolution temperature calculated was 1,151°C and the material was laminated at an average temperature of 1,155°C, considering the average discharge temperature of 1,215°C for this steel.

The model did not indicate precipitation of NbCN in the material at the temperature at which it was

Figure 4

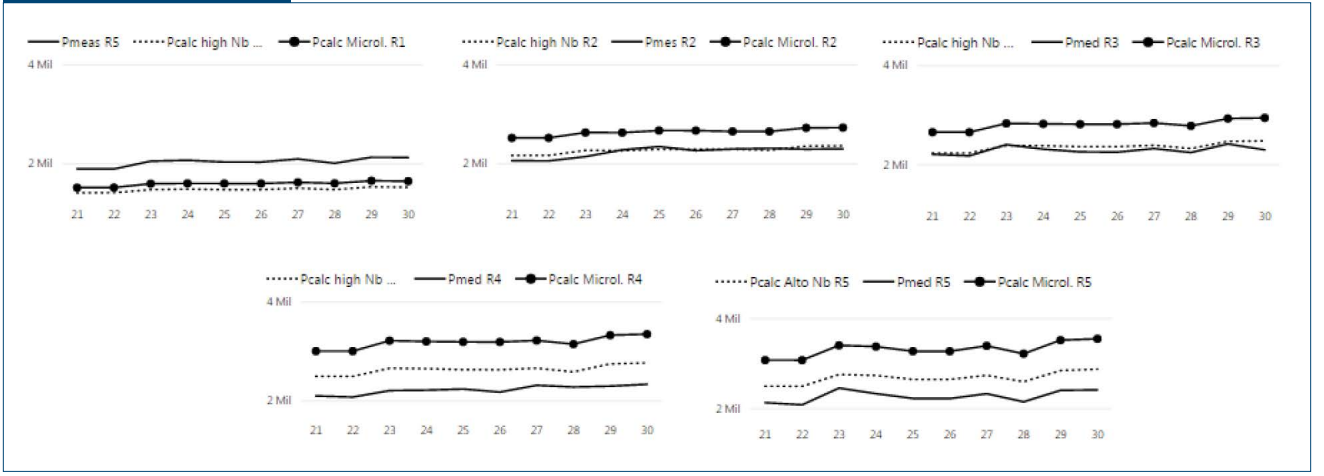

Comparison between roll force measured x calculated by the model using equations considering high-Nb steel and microalloyed steels for thickness of 38 mm. Unit of measurement of the graphs in tons.

Figure 5

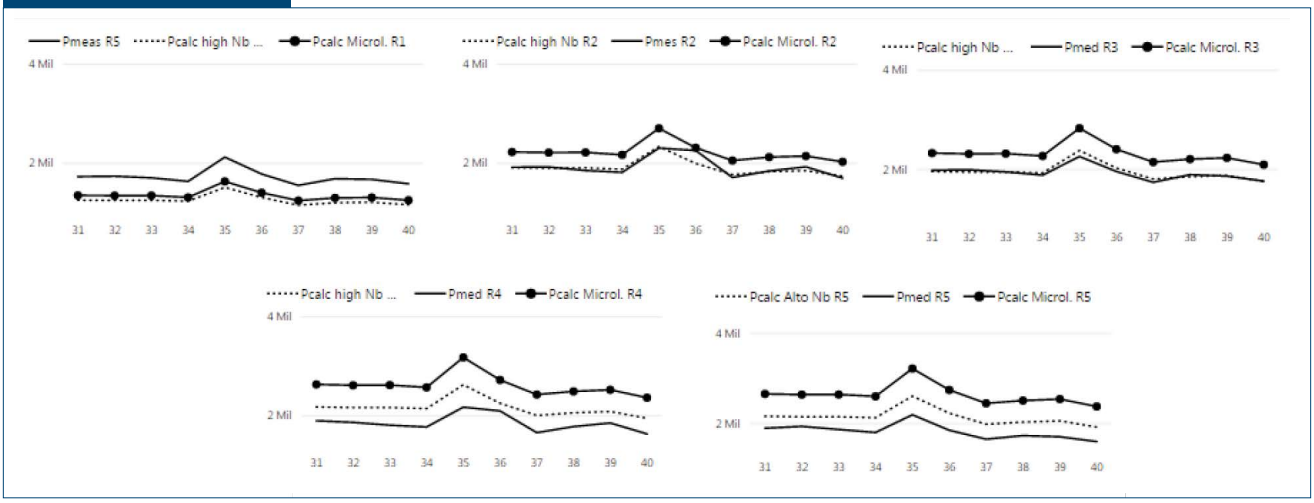

Comparison between roll force measured x calculated by the model using equations considering high-Nb steel and microalloyed steels for thickness of 40 mm. Unit of measurement of the graphs in tons.

Figure 6

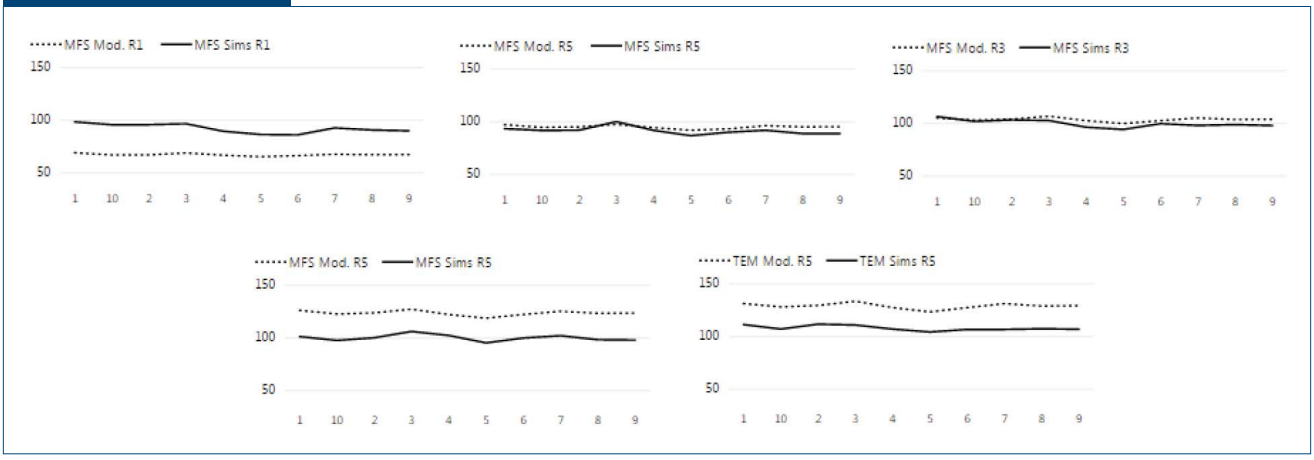

Comparison between actual mean flow stress (MFS) x calculated by model for thickness of 34 mm. Unit of measurement of the graphs in megapascal (MPa).

Figure 7

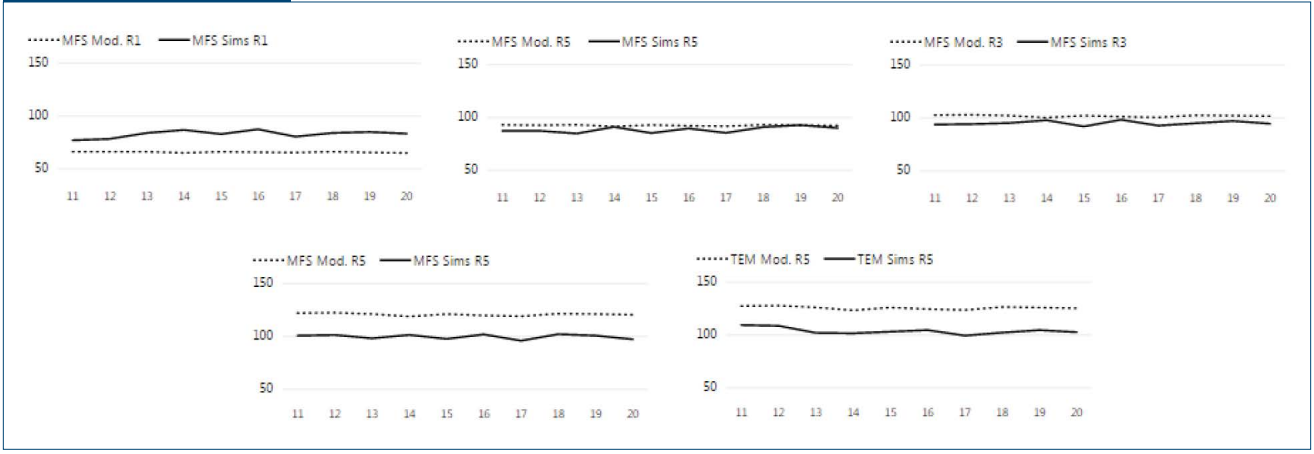

Comparison between actual MFS x calculated by model for thickness of 36 mm. Unit of measurement of the graphs in MPa.

Figure 8

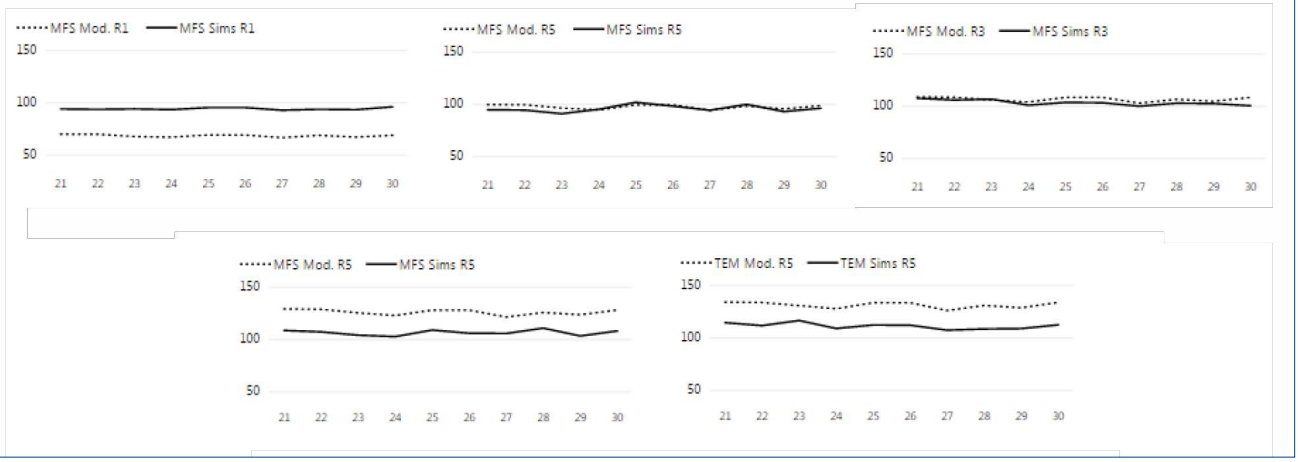

Comparison between actual MFS x calculated by model for thickness of 38 mm. Unit of measurement of the graphs in MPa.

Figure 9

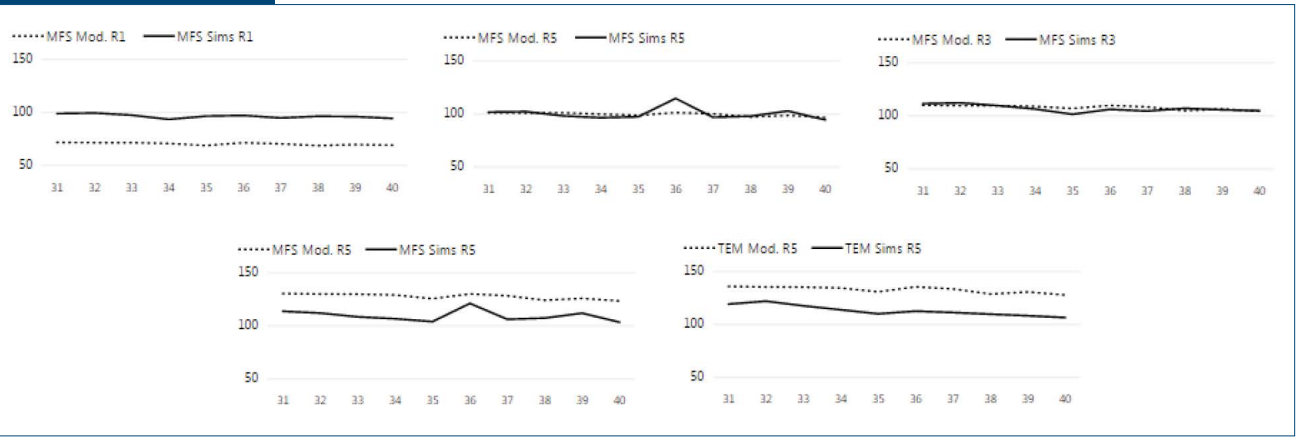

Comparison between actual MFS x calculated by model for thickness of 40 mm. Unit of measurement of the graphs in MPa.

laminated, a fact that would affect the increase of roll force. It is possible that there is precipitation of niobium during the roughing mill, but in a very small fraction not sensitive by model (less than 5%).

The austenitic grain size is consistent with that expected in this step of the hot strip lamination, the industry benchmark being a grain size between 80 and 120 µm, depending on the material.

Figure 10

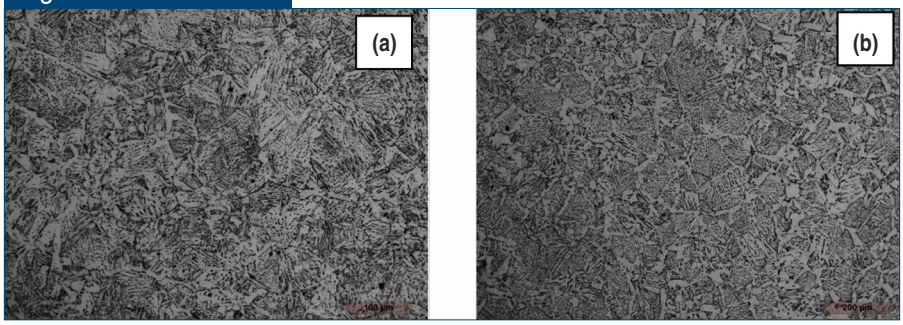

Microstructure along the specimen thickness, longitudinal section, with etching — optical microscope: a top-edge sample at 200x increase (a) and a tall specimen at 100x increase (b).

Conclusions

The model shows a good predictability of the roll force and MFS, because it followed the same trend of measured roll force and MFS for all coil thicknesses.

The equations used significantly influence the result of the force calculated by model, with the equations for high-Nb steel being more suitable in this case.

The microstructural evolution model shows a good predictability, which presented austenitic grain size consistent with the industry result.

The methodology used proved to be a good alternative for the company to perform optimizations in this stage of the hot rolling process.

Acknowledgments

The authors would like to thank ArcelorMittal Tubarão and Instituto Federal do Espirito Santo for providing the necessary production information and support for this study.

References

1. M.L.P. Machado, J. Denti and F. Fagundes, "A Thermomicrostructural Model for Simulation Disturbances in a Hot Strip Mill and Its Effect in Steel Properties, Roll Force and Exit Strip Thickness," *Latin American Journal of Solids and Structures,* Vol. 4, 2007, pp. 331–348.
2. R.G. Emanuelle, "Mathematical Model for Predicting Mechanical Properties in Hot Rolling Structural Profiles," dissertation, Universidade Federal de Minas Gerais, Belo Horizonte, Brazil, 2007.
3. F. Siciliano, "Mathematical Modeling of the Hot Strip Rolling of Nb Microalloyed Steels," Montreal, Canada: Ph.D Thesis, McGill University, 1999, p. 50.
4. L.V.R. de Carvalho and M.L.P. Machado, "Mathematical Model to Predict the Mechanical Properties of an Industrial Hot Rolled Round Bar Carbon Steel," *AISTech 2018 Proceedings,* Vol. III, 2018, pp. 2997–3004.
5. K. Minami, F. Siciliano, T.M. Maccagno and J.J. Jonas, "Mathematical Modeling of the Mean Flow Stress During the Hot Strip Rolling of Nb Steels," *ISIJ International,* Vol. 36, No. 12, 1996, pp. 1507–1515.
6. E.J. Palmiere, C.I. Garcia and A.J. Deardo, "Compositional and Microstructural Changes Which Attend Reheating and Grain Coarsening in Steels Containing Niobium," *Metallurgical and Materials Transactions,* Vol. 25A, No. 2, 1994, p. 277–285.
7. T. Gladman, *The Physical Metallurgy of Microalloyed Steels,* The Institute of Materials, London, U.K., 1997, p. 363.
8. A.F. Padilha and F. Siciliano, *Hardening, Recrystallization, Grain Growth and Texture,* (in Portuguese) 3rd ed., ABM, 2005. ✦

AISTech This paper was presented at AISTech 2019 — The Iron & Steel Technology Conference and Exposition, Pittsburgh, Pa., USA, and published in the Conference Proceedings.